Research Article

The Production of High Value Pig Iron Nuggets from Steelmaking By-Products – A Thermodynamic Evaluation

Daniel J. C. Stewart[a], David Thomson[b], Andrew R. Barron[a,c,d]*

[a] *Energy Safety Research Institute, Swansea University Bay Campus, Swansea, SA1 8EN, UK*

[b] *Tata Steel Strip Products UK, Port Talbot, SA13 2NG, UK*

[c] *Department of Chemistry and Department of Materials Science and Nanoengineering, Rice University, Houston, Texas 77005, USA*

[d] *Faculty of Engineering, Universiti Teknologi Brunei, Brunei Darussalam*

KEYWORDS: ironmaking; pig iron nugget; recycling; basic oxygen steelmaking dust; blast furnace dust

ABSTRACT

Zinc contaminated steelmaking by-products such as blast furnace (BF) dust and basic oxygen steelmaking (BOS) dust present a significant recycling challenge at integrated steelmaking plants. Rotary Hearth Furnaces (RHFs) provide an attractive route for recovery of Fe and Zn from these materials through carbothermal reduction of the oxides in the material to yield Direct Reduced Iron (DRI) and crude zinc oxide. The next generation of RHF processes such as ITmk3 and e-nugget produce pig iron nuggets from iron ore concentrates and coal, as iron and gangue separate *in-situ* without an additional melting unit. A computational study of the metal-slag system using FACTSAGE 7.3 suggests that production of pig iron nuggets of good quality (93.75 wt.% Fe, 4.3 wt.% C, 0.116 wt.% S, 0.66 wt.% Mn) can be produced from BF dust and BOS dust in a ratio of 37:63 with addition of 5.4 wt.% SiO_2 and 1.51 wt% MgO at 1450 °C. These computational results are in good agreement with experimental studies on similar material and, as such, suggest a practically feasible process.

1. Introduction

Iron rich by-product dusts and sludges are an unavoidable consequence of ironmaking and steelmaking activity. The recycling of these fine dusts is usually simple, reincorporating the material into the process through agglomeration in a sinter plant (Umadevi et al., 2013) or via cold bonded briquetting/pelletization (Andersson et al., 2019); however, dusts recovered from the off-gas dedusting systems in the blast furnace (BF) and basic oxygen steelmaking (BOS) plants at integrated works are often contaminated with zinc. The deleterious effect of zinc on the blast furnace is well known (Besta et al., 2013; Narita et al., 1981) and even relatively low concentrations of zinc (100-120 g Zn per ton of hot metal) in feedstock material can have negative effects on process stability and thus the economics of production. The removal of zinc from steelmaking materials via hydrometallurgical means (Cantarino et al., 2012; Jha et al., 2001; Oustadakis et al., 2010; Shawabkeh, 2010; Trung et al., 2011; Zhang et al., 2017) and pyrometallurgical means (Abdel-Latif, 2002; Assis, 1998; Brocchi and Moura, 2008; Mombelli et al., 2016a; Stewart and Barron, 2020) is well documented but these materials are often still stockpiled and underutilized by steel producers. Landfilling of these materials is not a long term economically and environmentally sustainable solution. The steel industry and the governments of countries the industry operates within are actively looking to avoid the negative environmental consequences of huge stockpiles of solid waste on defunct steel manufacturing sites, that must be remediated at huge expense before the land may be reutilized, as has been the case in many high profile plant closures (ENDS Report, 1992). Pyrometallurgical separation of zinc from these dusts in an on-site rotary hearth furnace (RHF) is becoming more commonplace at newer integrated works. These facilities utilize carbon in coal or in the by-products themselves to reduce, volatilize and capture the zinc from the materials in the form of a crude zinc oxide.

The major advantage of a carbothermal reduction route such as the RHF is the iron product is partially reduced and is known as direct reduced iron (DRI). High quality DRI can be >90% metallized (McClelland and Metius, 2003) and charging DRI back to the BF can reduce the coke rate of the furnace, which carries an economic and environmental benefit (Chatterjee, 2012). Unfortunately, DRI produced from recycled materials is often limited in

quality. High gangue content due to the nature of the input materials is inevitable and carries penalties such as increased slag volumes, but another key value driver of DRI is sulfur content. As DRI is substantially metallized, it can also be used to displace scrap within a BOS vessel or an electric arc furnace (EAF). Scrap steel is substantially more expensive per unit of iron than virgin ore (Yellishetty et al., 2011) and DRI that is of high enough quality to be recycled to the BOS vessel rather than the BF will have substantially higher value in use (VIU) to the steelmaker.

The BOS process is sensitive to sulfur addition in the scrap charge, because despite the presence of a basic slag, the high oxygen activity in the converter makes the dissolution of sulfur into the hot metal (HM) thermodynamically favorable (Schrama et al., 2017). Many high-performance steels require extremely low levels of residual sulfur within the HM, with the production costs sharpening steeply as ultralow sulfur concentrations (<0.001 wt.%) become necessary (Pehlke and Fuwa, 1985). As such, low sulfur scrap substitutes are expensive and thus low residual sulfur levels within DRI are desirable for the DRI producer.

Next generation RHF processes such as ITmk3 go one step further than the purely solid-state reduction of iron oxides. Through careful manipulation of slag chemistry, the iron in the ITmk3 process is sufficiently carburized to liquify and coalesce into pig iron nuggets (Fig. 1), completely separate from an immiscible, liquid slag phase (Kikuchi et al., 2010; Kobe Steel ltd, 2010). Similar nugget making processes include E-Iron, which uses an adapted linear tunnel furnace to produce iron nuggets from non-zinc bearing mill wastes (Simmons, 2015) and Hi-QIP which uses an un-agglomerated feed on a bed of carbonaceous reductant (Ishiwata et al., 2009). The production of pig iron nuggets from zinc bearing mill wastes has been reported previously (Birol, 2019; Wang et al., 2010; Zhao et al., 2012), implying the feasibility of the production of nuggets based on experimental laboratory conditions in inert gas atmospheres.

Fig. 1. Iron nuggets produced via a large scale ITmk3 pilot plant (Kikuchi et al., 2010). Reproduced with permission from the Kobe Steel Engineering Report Editorial Board.

Sulfur control in DRI production is mostly achieved by raw material input. DRI produced using coal as a reductant is too high in sulfur (0.44 wt%) to be utilized in a BOS/EAF melt shop (Seetharaman, 2014) and thus is usually utilized via a blast furnace, which is less sensitive to sulfur. However, the addition of a melting step and a molten slag, such as in ITmk3, offers an opportunity to sequester sulfur from the metallic iron within a distinct slag phase. This is not dissimilar to the mechanism by which sulfur is removed within the blast furnace (Schrama et al., 2017). Another potential avenue to add value to iron nugget production is by the simultaneous reduction of manganese oxides often found in BOS dust in small, but not insignificant amounts, into the pig iron nugget product (Longbottom et al., 2016; Mombelli et al., 2016a). Manganese is a common alloying element in the production of steel and is often added on a supplementary basis with the scrap charge to a BOS vessel or EAF in the form of ferromanganese alloys. This is a cost to the steel producer, therefore simultaneously reducing Mn into the hot metal produced during pig iron nugget making would be economically desirable. Srivastava reported the reduction of Mn_xO_y to the liquid iron phase during nugget making reactions using a manganiferous ore with minimal losses of Mn to the slag phase (18% at 1450 °C for 40 minutes) (Srivastava, 2014). However, this was performed using a high manganese iron ore rather than with steelmaking by-products and used graphite and polyethylene as a reducing agent.

Herein we propose that an exploration of the thermodynamics of the complicated slag-iron system present in nugget production, the ability for the nugget making process to desulfurize the produced pig iron and reduce manganese into the hot metal at a range of temperatures, slag chemistries and reductant levels can be determined. Three conditions need to be met to produce pig iron nuggets in a manner similar to the ITmk3 process or E-Iron;

- a low liquidus temperature slag, to allow for molten iron droplets to coalesce,
- sufficient carbon to reduce iron and zinc oxides to their elemental form, and
- sufficient carbon to further carburize the metallic iron such that the melting point is low enough to form molten pig iron at the reaction temperature.

Using BF dust and BOS dust from Tata Steel Port Talbot in the United Kingdom as a case study, the effect of various blends and temperatures is explored with respect to the thermodynamics of the chemical system. The study is limited in its scope to thermodynamics, without exploring the complicated reaction kinetics of the multiphase system and a comparison is made to experimental studies from literature performed on similar material. By comparing results of a thermodynamic study such as this to the experimental observations made in the literature to determine whether the relatively short reaction times in pig iron nugget making (<60 minutes) are sufficient to allow the slag-metal system to reach equilibrium or whether kinetic factors play a substantial role in determining Fe yield and Mn/S partition between the hot metal and the slag.

2. Methods

Calculations were performed using the *equilib* module of FACTSAGE 7.3. This module uses the Gibbs free energy minimization method to determine the equilibrium composition of complex heterogeneous systems. The input chemistry of the model for BOS dust and BF dust is shown in Table 1, based on material obtained from Tata Steel Port Talbot UK. Reducible oxygen associated to the iron within the material is denoted by O_{Fe}. For equilibrium calculations, all pure solid and gaseous species possible from the input chemistry were considered, as well as all applicable solid-state solutions from the FTOxid database. For the liquid phase two alloy solutions were considered from the FSstel and FToxid databases,

FSstel-liqu#1 to as the molten pig iron phase and FToxid-SLAGA#1 as the molten oxide slag system formed from the gangue. Phase diagrams were generated using the phase diagram module of FACTSAGE 7.3, using FToxid-SLAGA#1 as the target alloy solution phase for thermal projections. The equilibrium composition calculations are normalized to 100 g of input material. For clarity's sake in Figures, the FSstel-liqu#1 liquid alloy solution is referred to as 'Pig Iron' and the FTOxid_SLAGA#1 liquid alloy solution is referred to as 'Slag'.

Table 1

Chemical composition of the two zinc contaminated steelmaking by-products BF dust and BOS dust.

Material	Chemical composition (wt%)												
	Fe	SiO_2	Al_2O_3	TiO_2	$CaCO_3$	CaO	MgO	P_2O_5	MnO	S	ZnO	O_{Fe}	C
BF dust	26.79	5.61	2.63	0.14	6.89	0.77	0.159	0.62	0	0.62	0.87	14.41	40.49
BOS dust	59.14	2.31	0.34	0.06	13.08	4.44	1.16	0.088	0.74	0.001	4.14	14.50	0

3. The conditions of nugget making

3.1. Low liquidus temperature slag

The Al_2O_3-SiO_2-CaO-FeO system is well studied, due to its usefulness in describing the behavior of slags within the blast furnace. In blast furnace ironmaking, siliceous ores are fluxed with limestone to reduce the overall liquidus temperature of the gangue to encourage lower temperature separation from the iron (Geerdes et al., 2015).

The calculated ternary phase diagram of the SiO_2-CaO-Al_2O_3 system is shown in Fig. 2 The projection shows the liquidus projection front at temperatures 1000-1800 °C, at atmospheric pressure. The minimal liquidus temperature for this system as described is 1184 °C. It can be seen from Fig. 2 that the CaO-Al_2O_3-SiO_2 system for BF dust alone, 1700 °C > $T_{liquidus}$ > 1600 °C. For BOS dust the system is not molten even at 1800 °C. The solid line between the two points indicates the composition of the system as the ratio of BOS dust to

BF dust is changed. This line passes through regions of much lower liquidus temperature (~1200 °C) at a ratio of 2:1 BF dust to BOS dust.

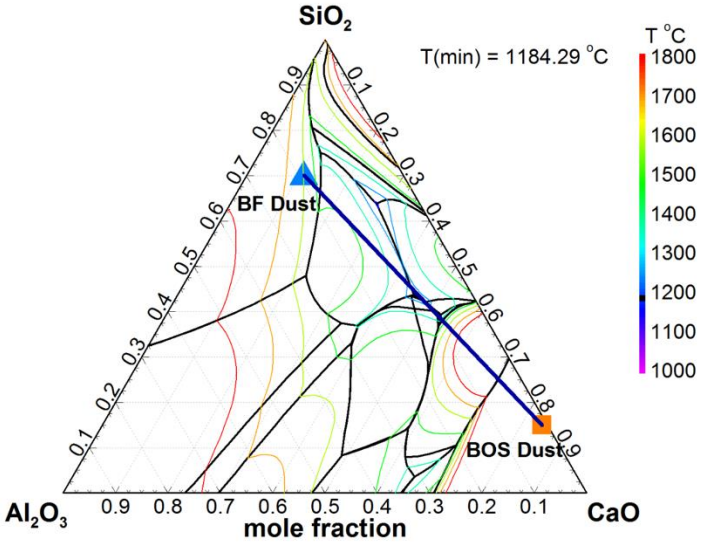

Fig. 2. Ternary phase diagram of the CaO-Al_2O_3-SiO_2 oxide system. Liquidus projection lines from 1000 – 1800 °C indicate under which compositions the oxide system is molten. The composition of BF dust and BOS dust are marked. For interpretation of the references to color in this figure legend, the reader is referred to the online version of this article.

FeO has a fluidizing effect on the CaO-Al_2O_3-SiO_2 as can be seen in Fig. 3. The minimum liquidus temperature of the system decreases dramatically with increased FeO addition, and at 0.2 mol fraction FeO the minimum liquidus temperature is 1013 °C, a substantial decrease from the pure CaO-Al_2O_3-SiO_2 system.

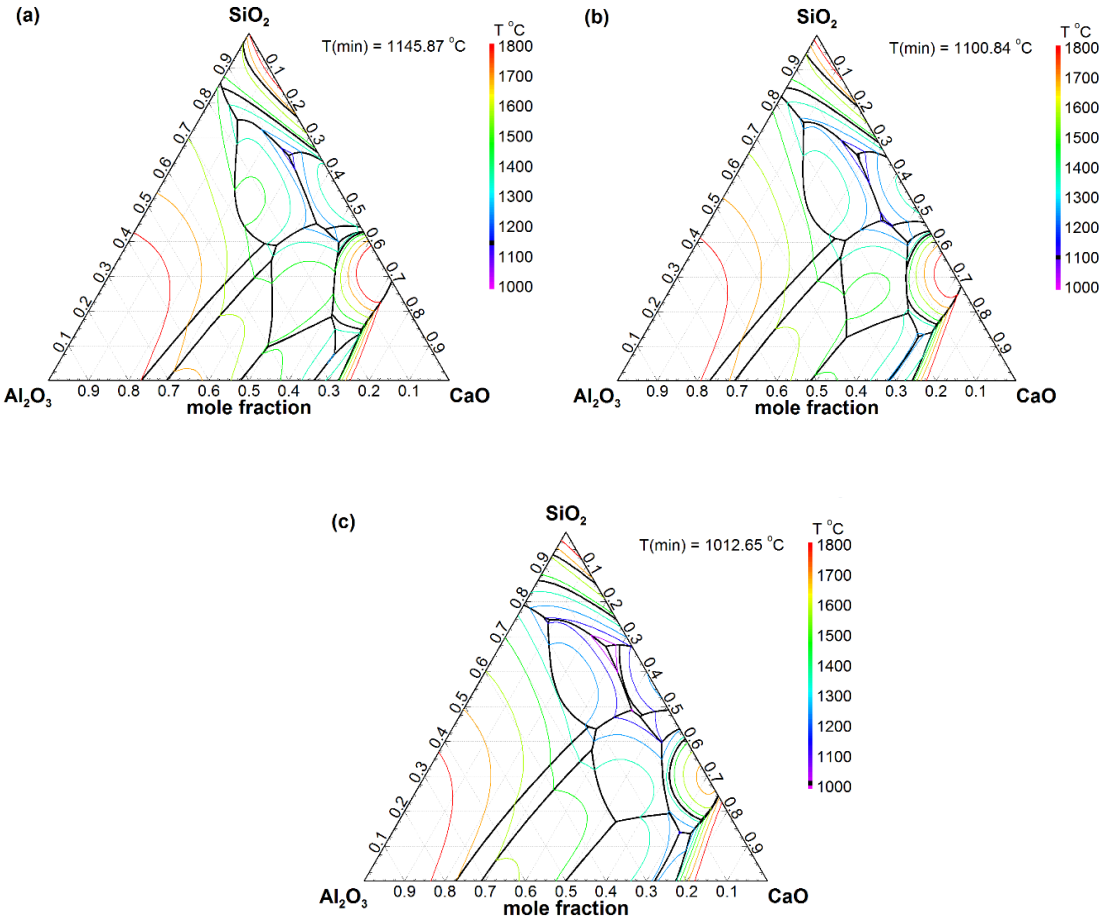

Fig. 3. Liquidus projections between 1000 °C – 1800 °C of the calculated temperature dependent CaO-Al_2O_3-SiO_2-FeO system at fixed FeO mole fraction compositions of (a) 0.05, (b) 0.1 and (c) 0.2. For interpretation of the references to color in this figure legend, the reader is referred to the online version of this article.

As the reduction of FeO occurs during the iron nugget making process occurs, the activity (concentration) of FeO within the slag phase will reduce and liquidus temperature of the slag system will increase as the reduction reactions progress. There is a trade-off in processing iron nuggets to allow for some FeO to remain within the slag post-reduction, increased slag fluidity may reduce the demand for auxiliary fluxing agent additions, lower theoretical plant operating temperatures and promote the kinetics of slag-metal desulfurization reactions which are diffusion controlled (Feild, 1917). These benefits are of course offset by the loss of iron, the primary product of iron nugget making to the slag phase.

3.2. Carbonaceous reduction of ferrous and zinc oxides

The role of carbon in the reduction of iron oxide and zinc oxide with regards to the processing of zinc bearing steel plants dusts has been recently reviewed (Stewart and Barron, 2020). BF dust has a super-stoichiometric amount of carbon present within the material with regards to reduction, even after reducing the Fe and Zn oxides in the material there is substantial remaining carbon. This can be seen clearly in Fig. 4 showing equilibrium iron species compositions of BF dust at increasing temperature. As T increases carbon reacts with the iron oxides present in the dust to form FeO at 650 °C, the iron is fully reduced to it's metallic form at 700 °C. Due to the large excess of carbon the iron completely carburizes to Fe_3C at 850 °C before melting at around 1050 °C. A small proportion of the molten slag phase is present between 450 °C and 1050 °C due to the fluidizing effects of FeO but as the reduction proceeds and more Fe is stripped from the slag phase into the molten pig iron phase it solidifies as the liquidus temperature increases. The calculations in Fig. 4 suggest a large proportion of solid carbon is still present within the system even at 1800 °C, indicating the liquid pig iron phase is saturated with carbon.

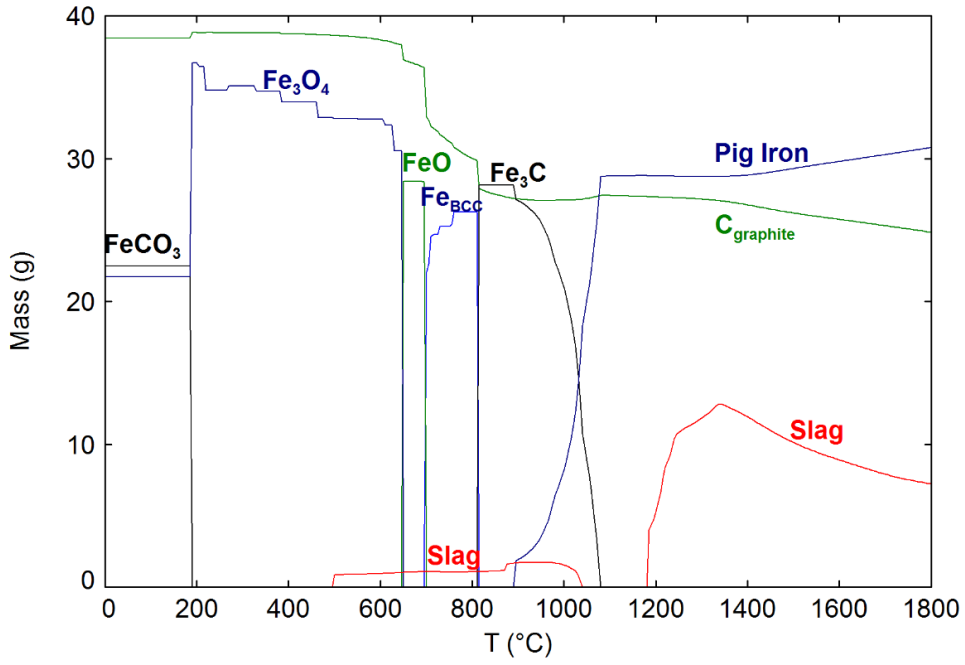

Fig. 4. The reduction of iron oxides within BF dust from 0 °C to 1800 °C. Pig iron and slag are both liquid phases.

Fig. 5 explores the behavior of zinc up to a temperature range of 1800 °C. The calculations indicate that zinc is present within the dust in the form of sphalerite (ZnS) at ambient conditions, this is in conflict with experimental characterization of the dust (Zeydabadi et al., 1997), which suggests it is present in the zinc oxide form in the material as received. It is likely as T increases the ZnO present at ambient conditions would react to form ZnS as a high excess of carbon and the presence of Fe_2O_3 promote sulfidation of zincite during roasting (Han et al., 2017). Studies of the sulfidation of ZnO using FeS as a sulfidization agent and demonstrated experimentally at temperatures > 450 °C (Zheng et al., 2018) suggests that ZnS would indeed form preferentially to FeS during the heating of BF dust as ZnO reacts with sulfur present in the material.

It is observed that a small proportion of ZnS dissolves within the molten slag phase present at T >450 °C, however the dissolved ZnS is shown to precipitate from the slag at around 875 °C. As T increases above 900 °C ZnS reduces and the zinc vaporizes, with the high residual carbon in BF dust at these temperatures sufficient to suppress the reoxidation of Zn to ZnO as oxygen activity is sufficiently low.

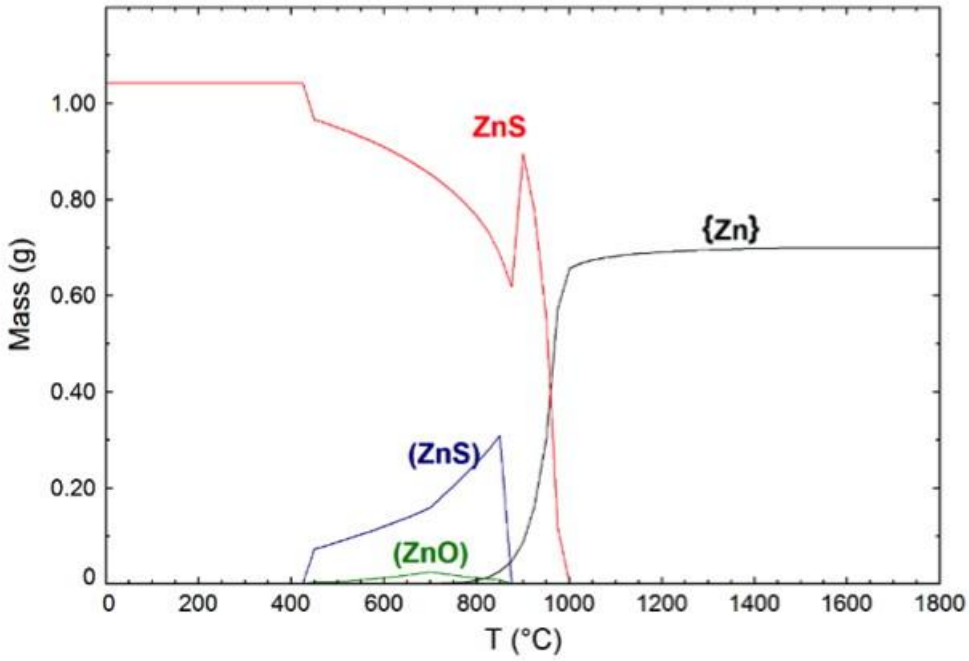

Fig. 5. The reduction of zinc within BF dust from 0 °C to 1800 °C. Round brackets ( ) are used to denote substances dissolved within the molten slag phase, curled brackets { } are used to denote substances in the gas phase and brace-less substances are solid.

During the heating of BOS dust as shown in Fig. 6 however, the lack of reductant sees most of the Fe dissolving into the molten slag phase in the form of FeO. Therefore, the yield of pig iron from heating BOS dust alone would be very low. The high activity of FeO within this system means the molten slag phase is formed at low temperatures (~1000 °C) Without the excess of C it can be observed that the molten pig iron phase does not form until the melting point of elemental iron (1538 °C) as there is negligible amounts of carbon dissolved within the metallic iron.

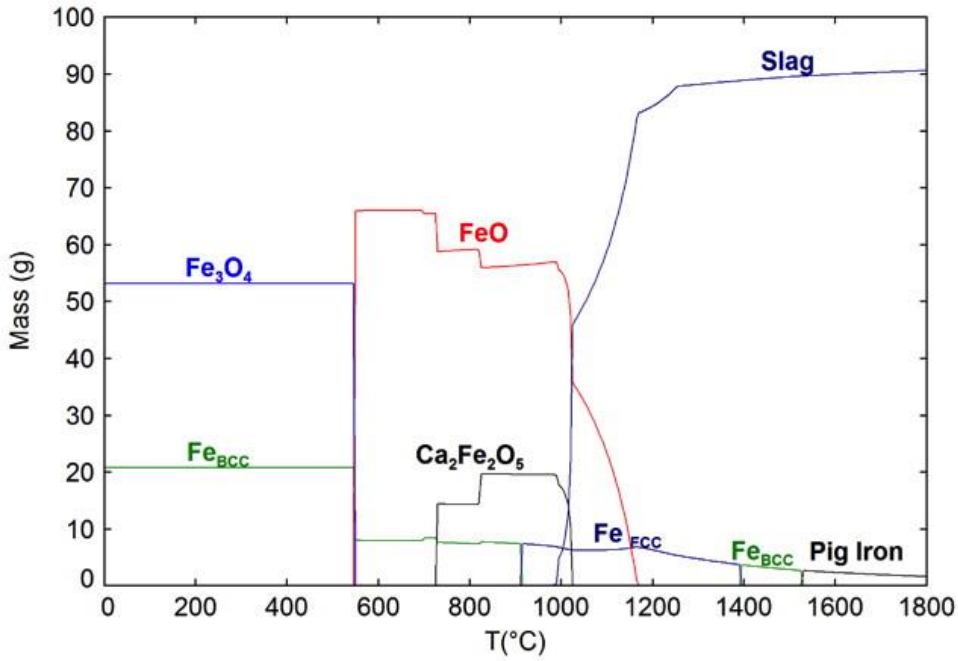

Fig. 6. Calculated equilibrium composition of BOS dust from 0 °C to 1800 °C.

Fig. 7 shows the heating of BOS dust along with the addition of a super stoichiometric amount of carbon (3 mol. per 100g of material). This addition of carbon suppresses the formation of the molten slag phase through the reduced activity of FeO and causes a large amount of solid CaO gangue to be present even at 1800 °C.

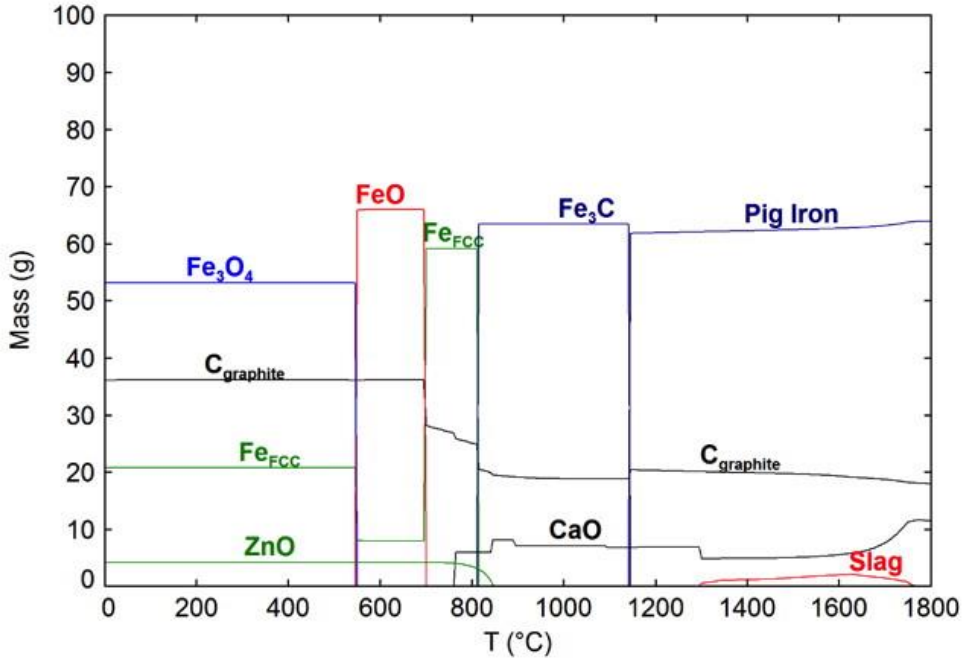

Fig. 7. Calculated equilibrium composition of BOS dust with the addition of 3 mol of carbon from 0 °C to 1800 °C.

An excess of carbon being present post-reduction can inhibit the coalescence of molten iron droplets in pig iron nugget production as observed during experimental studies (Han et al., 2015). It has been reported that work producing pig iron nuggets from jarosite waste and BF dust, with large excesses of carbon being detrimental to the coalescence of liquid iron droplets (Mombelli et al., 2019). Therefore, it is worth focusing on the optimum blend of BF dust to BOS dust to optimize for minimizing the solid fraction of the mixture at realistic process temperatures.

4. Varying the ratio of BF dust to BOS dust in pig iron nugget production

4.1. Iron recovery

Iron recovery is effectively the molar yield of the iron nugget making process. Some iron loss to slag in the emulsion loss (iron droplets unable to coalesce to a size separable from the immiscible slag phase) is an evitability and controlled by kinetic factors such as reaction time, but in this context solely represents the solubility of Fe in the slag phase at a given BF dust: BOS dust ratio and temperature.

Iron recovery is calculated using Eq. 1, with losses occurring either by the incomplete melting of the system or via dissolution of unreduced FeO into the slag.

$$R_{Fe_{\%}} = \left(\frac{Fe_{Pig\ Iron}}{Fe_{Pig\ Iron} + Fe_{Slag}}\right) \times 100 \quad (1)$$

Fig. 8 shows the effect of temperature (T) and BF dust fraction on the recovery of Fe. Once a stoichiometric amount of carbon is present in the blend at 0.35 BF dust fraction, iron recovery sharply increases, above 90% even at lower temperatures around 1100 °C. This seems to be a general behavior in the production of iron nuggets from a broad range of iron-bearing materials, with practical studies reporting the requirement of a stoichiometric amount of carbon relative to the total reducible oxygen content to produce iron nuggets with a high yield (Anameric et al., 2006; Archambo and Kawatra, 2020; Birol, 2019; Han et al., 2015; Mombelli et al., 2019, 2016a)

Following the reduction step only a small excess of carbon is required to saturate the Fe and subsequently melt it. However, the addition of an excess of BF dust leaves significant unreacted C in the system which as well as reducing productivity of nuggets from a kinetic viewpoint, also reduces the total iron loading to the furnace and therefore reducing throughput.

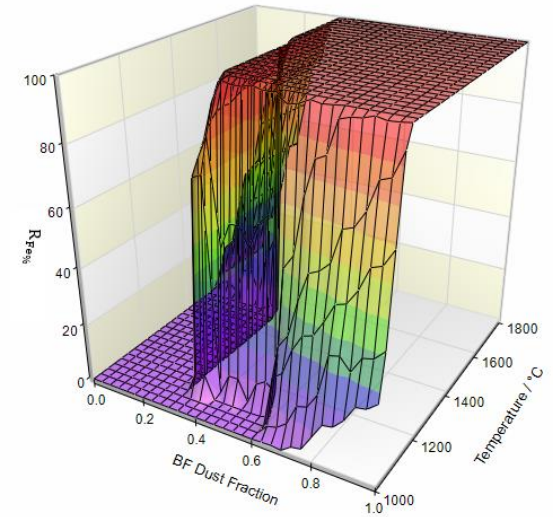

Fig. 8. Surface plot showing $R_{Fe_{\%}}$ at varying ratios of BF dust to BOS dust from 0 °C to 1800 °C.

Iron output is calculated from Eq. 2 and a 3D surface plot of output against BF dust fraction and T is shown in Fig. 9.

$$Fe_{Out}\% = \frac{R_{Fe\%} \times Fe_{Tot}}{100} \quad (2)$$

It is clear that the maximum iron throughput is achieved by heating to >1150 °C with a BF dust fraction of 0.35 but this productivity drops off as increasing BF dust is added to the system as the overall amount of Fe in the system decreases.

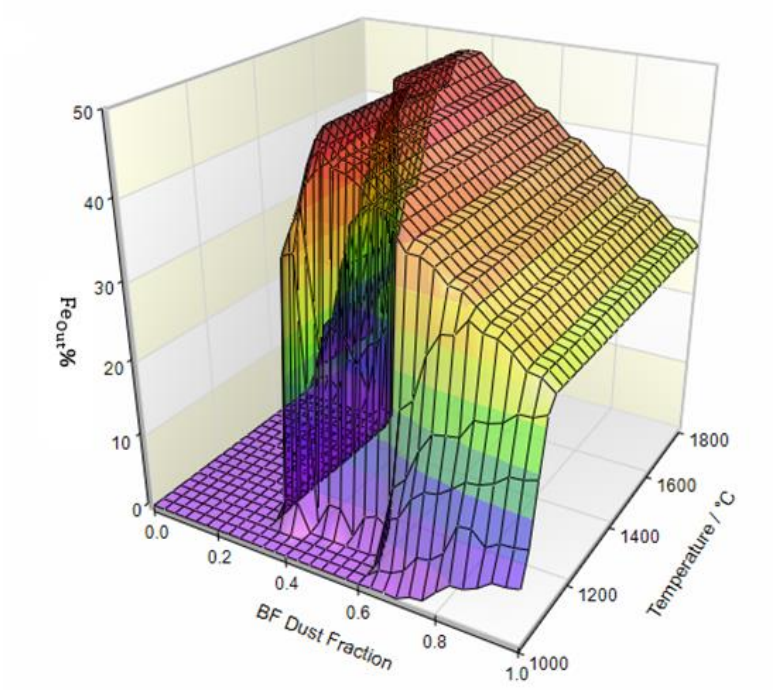

Fig. 9. Calculated surface plot showing Fe_{Out} at varying ratios of BF dust to BOS dust from 0 °C to 1800 °C.

4.2. Carburization

The carbon content of the produced pig iron is of relevance for two reasons. Firstly, as already established, a greater degree of carbon dissolved within the pig iron phase reduces melting temperature and therefore lowers the energy demand of the process. Secondly, increased carbon content in the produced nuggets has process benefits for the EAF/BOF meltshop (Memoli, 2015; Wei et al., 2019). It has been established that the critical role carburization plays in low temperature pig iron nugget making, showing that the separation of

slag and metal phases in the process was controlled by the rate of carbon dissolution into the newly formed metallic iron (Anameric et al., 2006).

To fully carburize the pig iron formed, carbon must be present in excess of the stoichiometric amount required for reduction of oxides such as Fe_2O_3 and ZnO as these reactions occur preferentially to carbon dissolving into metallic iron. Fig. 10 shows the changing carbon content calculated for the pig iron phase with relation to temperature and BF dust fraction. As expected, high temperature and BF dust fraction favor a degree of carburization of the pig iron, this is due to the high level of carbon present in BF dust compared to the negligible amount in the BOS dust. Very little carbon dissolves into the molten iron phase at low BF dust fractions (< 0.35), this is due to the amount of carbon in the system being insufficient to fully reduce the iron and zinc oxides. Once the BF dust fraction reaches a level at which carbon is in stoichiometric excess relative to the iron and zinc oxides in the system, further increase of BF dust fraction causes a sharp increase in the carbon content of the pig iron phase.

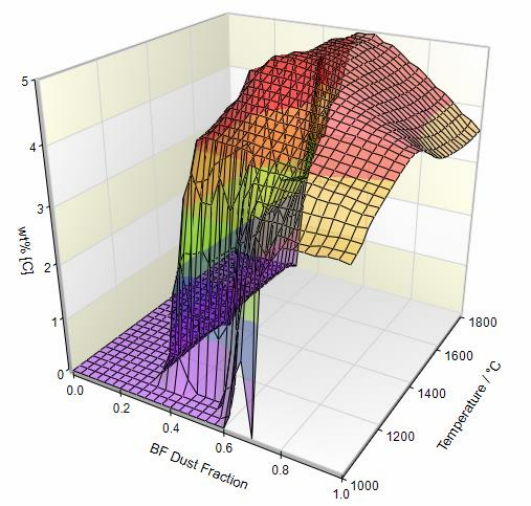

Fig. 10. Calculated surface plot showing the dissolved carbon (wt.% [C])in the pig iron alloy phase with varying BF dust fraction between 0 °C – 1800 °C.

4.3. Sulfur control

Due to BF dust containing substantially more sulfur per unit mass than BOS dust, as the BF dust fraction increases in the blend so too does S_{Tot} for the system. High temperature favors

the sequestration of S in the slag, while high BF dust fractions and low temperatures promote sulfurization of the pig iron. At BF dust fractions of 0.4 and 1200 °C the equilibrium sulfur content of the pig iron is 0.024 wt%, which reduces to 0.014 wt% at 1300 °C and 0.007 wt% at 1400 °C. This seems consistent with experimental observations of the S seizing capacity of ironmaking slags from literature increasing with T (Sosinsky and Sommerville, 1986; Taniguchi et al., 2012).

As the BF dust fraction increases, the overall basicity of the slag is reduced and therefore the activity of CaO is lowered. As such, S becomes less soluble in the slag phase and more so to the pig iron phase. It is therefore desirable to maintain a basic slag chemistry with regards to sulfur removal, but the drawback of this is the higher melting temperature of more basic oxide systems as discussed below.

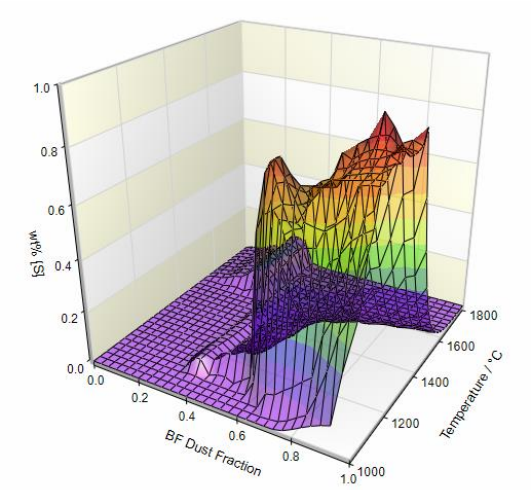

Fig. 11. Calculated surface plot showing the dissolved sulfur (wt.% [S]) in the pig iron alloy phase with varying BF dust fraction between 0 °C – 1800 °C.

4.4. Manganese recovery

Manganese reduction by solid carbon is feasible under standard conditions at 1417 °C (Srivastava, 2014) during the production of iron nuggets, but it is observed in this study that Mn dissolving into the pig iron is initiates once a stoichiometric amount of carbon in the blend is reached. This is likely due to the extremely low oxygen activity of the system once excess carbon is present as a solid in the system at equilibrium. At all temperatures with a BF dust fraction below 0.35 Mn is present either as solid MnO or in solution in the slag phase

(Fig. 12). The total amount of Mn in the system decreases with increasing BF dust fraction, hence the drop-off in wt% [Mn] as BF dust fraction exceeds the stoichiometrically optimal amount of carbon.

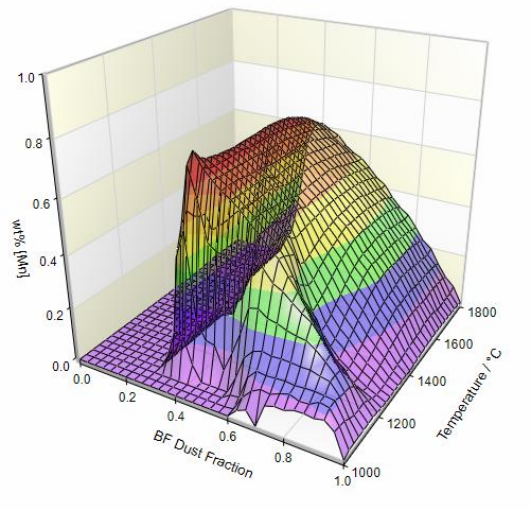

Fig. 12. Calculated surface plot showing the dissolved manganese (wt% [Mn]) in the pig iron alloy phase with varying BF dust fraction between 0 °C – 1800 °C.

4.5. Liquidity of the system

To facilitate the agglomeration of the molten pig iron phase into droplets large enough to separate easily from the slag by mechanical means, it is favorable that the system be as liquid as possible. As expected, higher temperatures lead to a decrease in solid fraction in the system. Fig. 13 shows the fraction of the system present as solids under the given conditions. The solid fraction is defined by Eq 3, where mass(s), mass(m), and mass(v) are the mass of material in the solid, molten and vapor phases, respectively.

$$\text{Solid Fraction} = \frac{\text{mass(s)}}{\text{mass(s)}+\text{mass(m)}+\text{mass(v)}} \quad (3)$$

The solids present in the system here can be classified as non-carbonaceous and carbonaceous. Carbonaceous material under these conditions is in the form of solid iron carbide Fe_3C and elemental carbon in the form of graphite. Non-carbonaceous material is all other solid matter, which includes gangue mineral oxides like Si, Ca and Al oxides,

unreduced iron oxides and metallic but un-melted iron. By plotting these two types of solid independently of one another, a clearer picture of the process can be obtained (Fig. 14).

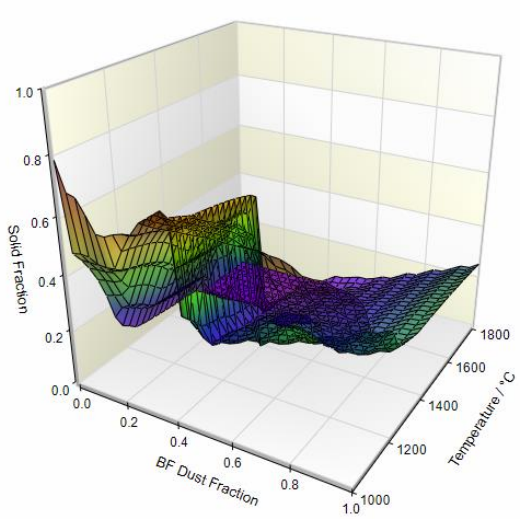

Fig. 13. Calculated surface plot showing the fraction of the system present as a solid with varying BF dust fraction between 0 °C – 1800 °C.

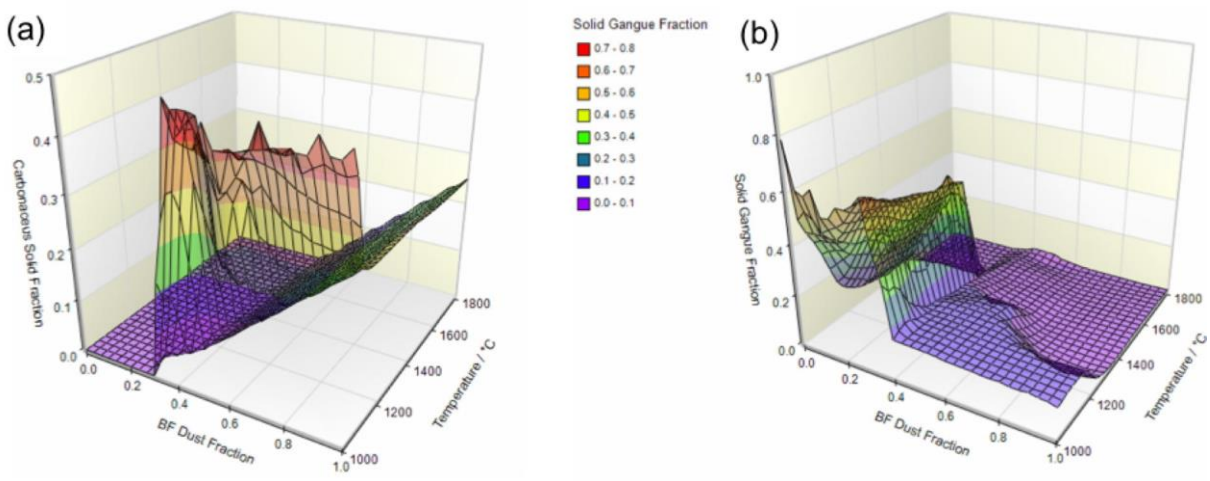

Fig. 14. Surface plots showing the fraction of the system present as solid carbonaceous material (a) and non-carbonaceous (b) with varying BF dust fraction between 0 °C – 1800 °C. For interpretation of the references to color in this Figure legend, the reader is referred to the online version of this article.

Large proportions of solid carbonaceous matter are only present in significant proportions at large BF dust fractions. The region confined between 0.4 – 0.6 BF dust fraction and 1000 °C – 1150 °C in Fig. 14a is due to the solid carburization of Fe to Fe_3C but at temperatures not sufficient to melt the iron carbide. It can be seen that at high temperatures

large amounts of solid graphite is present when the BF dust fraction is high. This is due to the pig iron phase being saturated with carbon and the low activity of oxygen means the carbon is not simply oxidized to form gases.

In Fig. 14 the solid non-carbonaceous material is present at low BF dust fractions and temperatures. As BF dust fraction moves from 0 to 0.3 the solid non-carbonaceous fraction begins to increase as FeO is reduced from the slag and the liquidus temperature of the CaO-SiO_2-Al_2O_3 system increases. The solid fraction drops substantially as the BF dust fraction exceeds 0.35, as iron is reduced and melts but at temperatures below 1500 °C the system still contains substantial calcium oxide minerals which would impede the coalescence of iron nuggets. Once the amount of carbon in the system exceeds the required amount to reduce all reducible oxides (Zn, Mn, Fe etc.) and carburize the iron, additional carbon would be detrimental to the productivity of the process.

5. Introduction of fluxing agents

As explored above, the optimum ratio to produce iron nuggets from BF dust and BOS dust appear to be in a proportion of 37:63. This provides sufficient carbon to reduce and carburize iron oxides present, reduces oxygen activity sufficiently to promote desulfurization and simultaneously recover Mn in the pig iron without incorporating excess carbon into the system which may impede the kinetics of production. However, the temperatures required to fully fluidize the gangue in the system to produce a molten slag are high, the system at these conditions is not fully liquid at 1450 °C. Limestone is often used as a flux to promote fluidization of the acidic silica impurities found in iron ore in blast furnace ironmaking, but at 37% BF dust: 63% BOS dust the gangue chemistry is very basic with a wt.% CaO/SiO_2 ratio of 2.59. As such the slag produced is fully saturated with CaO and excess amounts of CaO exists as a solid at nugget making temperatures of ~1450 °C. Two criteria must be met in order for nugget making to be feasible with regards to fluidizing the oxide gangue present. Firstly, the liquidus temperature of the gangue must be decreased sufficiently with additions to become molten at reaction temperatures. Secondly, the molten slag that is produced must be compatible with a refractory surface that is suitable for an RHF.

5.1. Flux additions

Under the assumption that all MnO and FeO is reduced from the slag, the slag system can be simplified to a CaO-SiO_2-MgO-Al_2O_3 quaternary system, and the temperatures at which this system is fully fluid can be projected via a phase diagram as shown in Fig. 15. To fluidize the system, SiO_2 can be added to the blend to flux the excess CaO and bring the liquidus temperature of the system down. It would be desirable to add only enough SiO_2 to form a slag that is only just CaO saturated, as a fully fluid slag with a high CaO activity would be favorable for the sequestration of S and P from the pig iron into the slag phase.

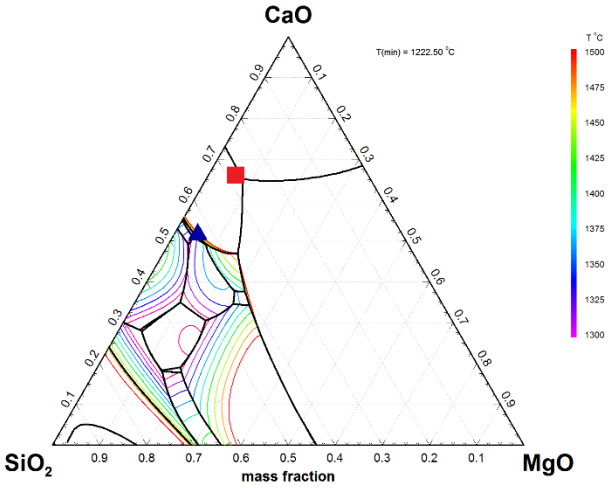

Fig. 15. Melting projection for the CaO-SiO_2-MgO-Al_2O_3 system at fixed 9 wt% Al_2O_3 between 1300 – 1500 °C. The red square corresponds to the CaO-SiO_2-MgO-Al_2O_3 composition in a 37:63 BF dust:BOS dust blend. The blue triangle corresponds to a blend with 3.307 wt% SiO_2 added. For interpretation of the references to color in this Figure legend, the reader is referred to the online version of this article.

Fig. 15 suggests that an addition of 3.307 wt% SiO_2 would be sufficient to fully fluidize the CaO-SiO_2-MgO-Al_2O_3 system for a 37:63 BF dust: BOS dust blend at proposed nugget making temperatures of 1450 °C. The phase diagram above, however, is limited to only four components. To consider all the components present in the BF dust: BOS dust mixture, the addition of SiO_2 to the 37:63 BF dust: BOS dust system is explored through FactSage's equilib module. Using the precipitate target function, it was determined that at 1450 °C the minimum SiO_2 addition required to flux the CaO present and generate a fully

molten slag was 5.4g SiO_2 per 100g of the blend. This which is in reasonable agreement with Fig. 15 but accounts for the interaction with the pig iron alloy as well as minor constituents not considered in the phase diagram such as TiO_2 and S which of course affect the slags properties.

Fig. 16 shows the effect that this SiO_2 addition has on the Mn, S and Si levels in the pig iron phase as this addition is made. The concentration of Si increases dramatically as SiO_2 is added to the mixture as expected, and S also increases with SiO_2 addition to 0.155 wt%; however, with only SiO_2 addition, this type of slag would be extremely aggressive to refractories. It is highly basic, meaning it would readily attack and dissolve acidic refractories. The slag is also not MgO saturated, meaning basic refractories such as those used on the slag line of a basic oxygen converter would also be attacked and corroded by this slag. Saturating slag with MgO is common practice in EAF and BOS steelmaking as a means of prolonging vessel lining lifetime (Bennett and Kwong, 2010; Song et al., 2020), by mitigating the interaction between the liquid slag and the basic furnace lining.

Beggs describes the mechanism of corrosion by the charge to an MgO refractory in an RHF in their 1969 patent for a vitrified refractory surface designed to impede corrosion by the aggressive FeO-SiO_2 liquid eutectic (Beggs, 1969). The unsaturated nature of the slag with respect to the MgO refractory allowed ingress of liquid into the surface, whereby thermal expansion causes catastrophic spalling. To mitigate this, the MgO capacity of the slag system was explored using Factsage's equilib function. Again, using the precipitate target function, calculations showed that 1.51 g MgO could be added to the system before it becomes saturated and a Merwinite, $Ca_3Mg(SiO_4)_2$, precipitate would begin to form with increasing MgO inclusion. This addition would render the slag less aggressive to an MgO or dolomite based refractory and thus prolong refractory lifetime in a production environment. Fig. 16b shows the effect this MgO addition has on dissolved elemental composition within the pig iron phase. The levels of dissolved Si in the Pig Iron dramatically decrease to 0.92 wt% and the MgO addition also resulted in a lower total of dissolved S in the pig iron phase. Mn levels in the pig iron were almost unchanged by the addition of MgO.

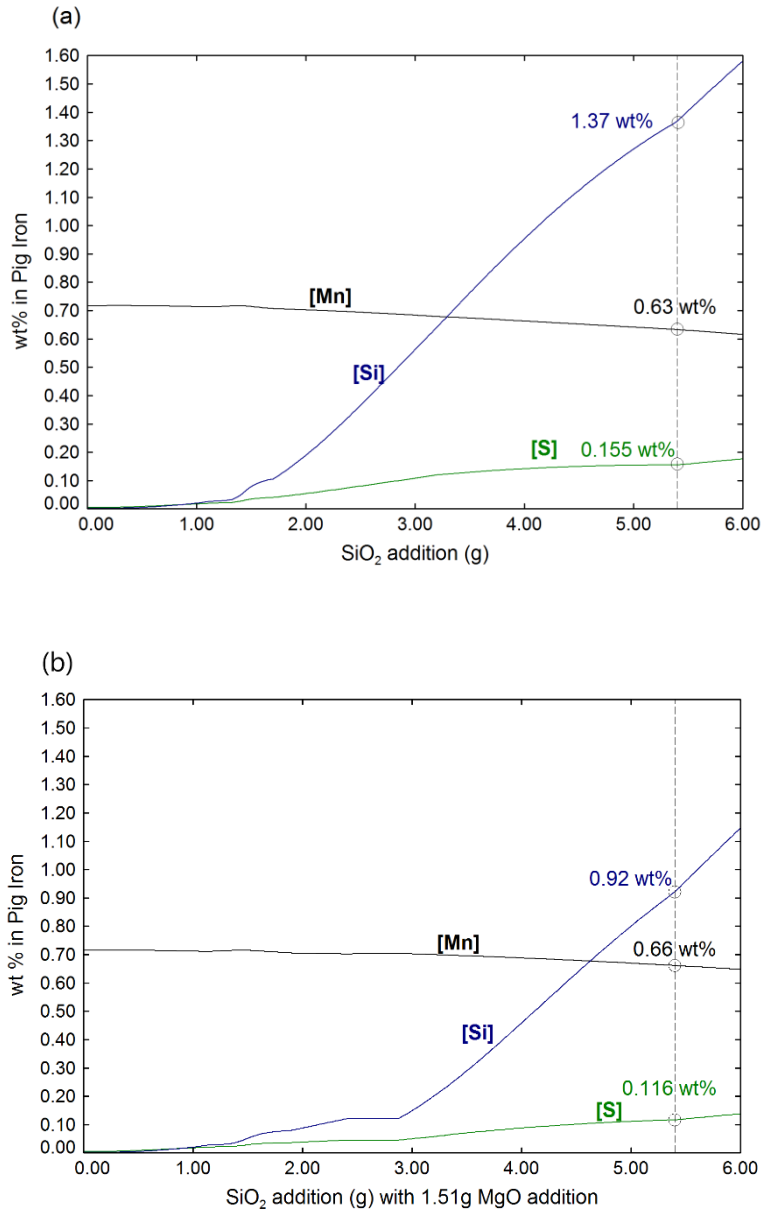

Fig. 16. Changing manganese, silicon and sulfur content of the pig iron phase with SiO_2 addition at 1450 °C with 0 g MgO added (a) and 1.51 g added (b). The dashed line corresponds to the saturation point of the slag, the minimum addition of SiO_2 needed to fully fluidize the system.

The calculated chemical composition of the pig iron nuggets and slag formed at 1450 °C with addition of 5.4g SiO_2 and 1.51g MgO per 100g of blend is shown in Table 2. The calculated pig iron sulfur content of 0.116 wt% S is relatively high meaning pig iron nuggets produced from waste would have to be utilized as part of a mix of scrap sources to supplement steel production, however their lack of gangue, complete metallization, high

carbon and manganese content and partial desulfurization would mean they have a higher value in use than DRI in a steel plant.

The present study is thermodynamic in scope to act as a guide for future experimental work to fully gauge the feasibility of processing BF dust and BOS dust in this manner; however, pig iron nuggets produced at similar temperatures in laboratory studies appear to be somewhat consistent with the results of this study, as shown in Table 3. These experimental studies suggest a reaction time of 15-20 minutes may be suitable to produce iron nuggets, though it appears higher total gangue content increases reaction times (Birol, 2019).

Table 2

Calculated pig iron and slag compositions at 1450 °C for 100 g 37:63 BF dust to BOS dust ratio with the addition of 5.4 g SiO_2 and 1.51 wt% MgO. Under these conditions the system is fully fluidized, the remaining balance of mass of the system is gaseous or a minor constituent dissolved into the slag and pig iron.

Calculated pig iron composition		Calculated slag composition	
Element	Composition (wt.%)	Phase	Composition (wt. %)
Fe	93.75	FeO	0.01
C	4.30	Al_2O_3	5.67
P	0.24	SiO_2	37.85
S	0.116	CaO	43.53
Si	0.92	MgO	10.95
Mn	0.66	Ti_2O_3	0.22
		SiS_2	0.61
		CaS	0.58
		MnO	0.18

The study by Wang et al. utilizes very similar methods to the ones suggested herein, demonstrating that using a basic Ca_2SiO_4 saturated slag to produce nuggets from BF dust and BOS dust is experimentally possible (Wang et al., 2010). The levels of S in the product pig iron nuggets are extremely low in that work however, and this may be related to a few factors. The input materials used in the work appear to have substantially lower S content than this study and the work of Birol et al. and a Ca_2SiO_4 saturated slag as used in the study has significantly better sulfur capacity than an acidic slag as used in the other studies (Birol, 2019).

Table 3

Comparison of input materials and pig iron nugget chemistry used in experimental studies.

Study	Materials	Temp. (°C)	Reaction time (min.)	Composition (wt.%)				
				Fe_{Tot}	C	Si	P	S
Ishiwata et al., 2009	Ore	1500	15	57.3	-	3.29	-	-
	Coal			-	85.7	-	-	0.54
	Pig iron nugget			Bal.	2.5	0.08	0.04	0.21
Birol, 2019	BF dust	1400	15	25.27	37.1	3.87	-	0.40
	Mill scale			66.19	-	0.26	-	0.01
	Pig iron nugget			94.8	3.24	0.259	0.0039	0.209
Wang et al., 2010	BOF sludge	1400	10	71.48	1.32	1.86	0.13	0.04
	BF dust			30.87	34.25	2.73	0.052	-
	Pig iron nugget			92.91	3.61	-	0.094	0.023

Most of the work that has been carried out producing pig iron nuggets from by-product dusts has focused principally on the properties of the pig iron nuggets produced,

while the chemistry and morphology of the slag generated has been somewhat neglected. Wang et al. reported iron content of slags for the purposes of calculating iron recovery but the mineralogical properties of the produced slag are not reported (Wang et al., 2010).

The Scheil-Gulliver solidification model is a useful tool for projecting the mineralogy of slags as they solidify (Durinck et al., 2007). The model assumes diffusion rates of infinity for the liquid phase and zero for the solid phase, which can limit the model's accuracy under circumstances such as extremely high viscosity liquid solidification.

Table 4

Scheil-Gulliver cooling projection for slag produced by addition of 37:63 BF dust to BOS dust with the addition of 5.4g SiO_2 and 1.51 wt% MgO. Phases <0.01 wt% have been omitted. The temperature of final disappearance of liquid slag was calculated to be 953 °C.

Phase	Formula	Calculated wt%
Åkermanite	$Ca_2MgSi_2O_7$	41.13
Merwinite	$Ca_3MgSi_2O_8$	39.90
Anorthite	$Ca_2Al_2Si_2O_8$	9.56
Gehlenite	$Ca_2Al_2SiO_7$	5.60
Calcium sulfide	CaS	1.53
Wollastonite	$CaSiO_3$	1.12
Perovskite	$CaTiO_3$	0.36
Spinel	$(Mg, Fe)(Al, Cr)_2O_4$	0.06
Diopside	$CaMgSi_2O_6$	0.03

Table 3. shows a calculated Scheil-Gulliver composition of the slag phase from the conditions set out in Table 2. to estimate the phase composition of the cooled slag product. The slag is predominately estimated to be comprised of merwinite, melilite minerals such as

akermanite and gehlenite, and anorthite. The lack of free periclase (MgO) and lime (CaO) in the cooled slag is desirable if the slag were to be utilized in the construction sector due to the volumetric stability issues posed by the formation of hydroxides from CaO and MgO (Fisher and Barron, 2019).

Microstructure of steelmaking slags is of great importance for the control of leaching of heavy metals which can render slags untenable for recycling. Mombelli et al. discussed the influence of microstructure on heavy metal leaching characteristics in electric arc furnace slag (Mombelli et al., 2016b), suggesting phases such as spinel and gehlenite suppress leaching of Ba, V and Cr from slag, while larnite (β–Ca_2SiO_4) is more prone to leaching metals. The method by which slag is cooled can also manipulate the mineralogy of the final product, and thus the leaching behavior (Strandkvist et al., 2020).

In order to develop a nugget making process from by-products with zero solid waste, slag leaching and weathering behavior will require more in-depth study to ensure a usable product.

5.2 Recovery of zinc

The quality of the zinc oxide produced from such a process is challenging to predict using a purely thermodynamic methodology, and often neglected in practical studies. Zhao et al. studied Zn removal rates in nugget production from steelmaking by-products (Zhao et al., 2012) but focused on removal rates from the iron rather than on the quality of the zinc oxide product. The bag filter dust from a RHF plant (sometimes referred to as secondary rotary hearth furnace dust) typically contains any volatile elements from the input material such as Zn, Pb, Cd, Cl, Na and K, and is therefore heavily dependent on the quality of input materials. RHF secondary dusts are usually collected by means of a dry fabric dedusting filter system in the off-gas treatment portion of the plant (Tsutsumi et al., 2010). In terms of recycling, elements such as Cl and Cd are considered impurities, and can be controlled through material input chemistry control.

One element that is also considered undesirable for zinc recyclers is iron (Antuñano et al., 2019), and contamination by this element is much more closely tied to the manner in

which a rotary hearth furnace is operated. Poor mechanical strength of pellets and fines generation during processing are the major contributors to iron contamination in the secondary dust product from an RHF. There does not appear to be any fundamental reason the secondary dust produced from an RHF producing iron nuggets would be significantly different in terms of quality than the secondary dust produced from an RHF producing DRI from recycled materials such as a Fastmet plant. A comparison between Waelz oxide (secondary dust from a Waelz kiln), secondary RHF dust and the off-gas product from producing nuggets from blast furnace dust in a laboratory study is show in Table 5.

Table 5

Comparison of secondary zinc containing dusts from a Waelz Kiln, RHF and a laboratory study producing iron nuggets from BF dust.

	Composition wt%								
Material	C	Fe	Zn	Pb	Na	K	Cl	SiO_2	Source
Waelz Oxide	0.5-1.0	3.1-5.4	55.0-58.0	7.0-10.0	0.1	0.1	4.0-8.0	0.-1.0	(Mager et al., 2000)
RHF secondary dust	-	3.73	22.78	-	7.92	12.77	-	2.23	(Liang et al., 2020)
Hi-QIP nugget production (laboratory scale)	0.68	6.66	47.1	7.02	0.22	1.95	13.2	0.2	(Sawa et al., 2001)

As can be seen in Table 5, the materials are quite variable but made up of similar elements. It is difficult to draw direct comparisons from the laboratory study to the industrially produced samples as production conditions will be dramatically different. It is worth noting however, that the Hi-QIP study was with a loose, agglomerated feed, which may go some way to explaining the higher iron contamination in the material from that work (Sawa et al., 2001). It is likely, based on the chemical composition of input material as well as the composition suggested by Sawa et al.'s study that a cleaning step would be required to

remove halides and soluble alkali metals such as Na and K as is common for waelz oxide (Mager et al., 2000) before the product is considered suitable for use in the production of zinc via electrowinning. It may be feasible to source SiO_2 from sustainable sources for the purposes of this work, this may include wastes from other industries such as coal fly ash (Yao et al., 2015) or rice husk ash (Srivastava et al., 2006). MgO could potentially be sourced from spent refractory linings from BOFs or EAFs (Horckmans et al., 2019) as an environmentally favorable alternative to virgin material.

This work suggests that modification of emerging RHF and linear tunnel furnace based may potentially be adapted to process zinc contaminated by-products, recovering a higher value pig iron nugget product than established DRI recovery routes such as FASTMET. Technical considerations such as refractory design, off-gas dedusting system design would require modification to accommodate high volatile metal content and a basic slag.

6.0 Conclusions

This study was undertaken to determine the feasibility of an adapted pig iron nugget process as a viable recycling route for BOS dust and BF dust from an integrated steel plant, from a thermodynamic perspective.

The main outcomes of the work are:

- The production of pig iron nuggets from steelmaking by-products is thermodynamically feasible at reasonable operating conditions of 1450 °C.
- The addition of SiO_2 and MgO as fluxing agents allows for a reduction in process temperature, and has benefits for control of sulfur sequestration by the slag phase
- Zinc from the input materials could be captured from the process as a crude oxide in a similar manner to FASTMET (McClelland and Metius, 2003) and sold to recyclers as an addition revenue source.
- SiO_2 and MgO used to supplement production via a pig iron nugget process could potentially be sourced from industrial by-products.

- Iron nuggets produced are of an appropriate quality to supplement scrap in BOS/EAF processes
- If the slag produced from such a process is found to be volumetrically stable, it may be utilized as an aggregate leading to a process with little to no solid waste generation.

To validate these results a full laboratory scale study must be conducted to explore the validity of the assumptions made in this work, as well as kinetic factors which will likely play a substantial role in the process.

Declaration of Competing Interest

The authors declare that they have no known competing financial interests or personal relationships that could have appeared to influence the work reported in this paper.

Acknowledgments

Financial support was provided by Materials and Manufacturing Academy (M2A) that has been made possible through funding from the European Social Fund via the Welsh Government, the Engineering and Physical Sciences Research Council (EPSRC), and Tata Steel Europe. Additional support is provided by the Reducing Industrial Carbon Emissions (RICE) operations funded by the Welsh European Funding Office (WEFO) through the Welsh Government.

Appendix A

Supplementary data associated with this article can be found, in the online version, at XXXXXXXXXX.

References

Abdel-Latif, M.A., 2002. Fundamentals of zinc recovery from metallurgical wastes in the enviroplas process. Miner. Eng. 15, 945–952. DOI:10.1016/S0892-6875(02)00133-4.

Anameric, B., Rundman, K.B., Kawatra, S.K., 2006. Carburization effects on pig iron nugget making. Miner. Metall. Process. 139 23, 139–150. DOI: 10.1007/BF03403201.

Andersson, A., Gullberg, A., Kullerstedt, A., Ahmed, H., Ökvist, L.S., 2019. Upgrading of blast furnace sludge and recycling of the low-zinc fraction via cold-bonded briquettes. J. Sustain. Metall. 5, 350–361. DOI:10.1007/s40831-019-00225-x.

Antuñano, N., Cambra, J.F., Arias, P.L., 2019. Hydrometallurgical processes for Waelz oxide valorisation – An overview. Process Saf. Environ. Prot. 129, 308–320. DOI:10.1016/j.psep.2019.06.028.

Archambo, M.S., Kawatra, S.K., 2020. Utilization of bauxite residue: recovering iron values using the iron nugget process. Miner. Process. Extr. Metall. Rev. 7508. DOI:10.1080/08827508.2020.1720982.

Assis, G., 1998. Emerging pyrometallurgical processes for zinc and lead recovery from zinc-bearing waste materials. Zinc and Lead Processing Symposium, The Metallurgical Society of CIM, Calgary, Canada, August 1998.

Beggs, D., 1969. Furnace Hearth. US Patent 3,452,972.

Bennett, J., Kwong, K.S., 2010. Thermodynamic studies of MgO saturated EAF slag. Ironmak. Steelmak. 37, 529–535. DOI:10.1179/030192310X12706364542669.

Besta, P., Janovská, K., Samolejová, A., Beránková, A., Vozňáková, I., Hendrych, M., 2013. The cycle and effect of zinc in the blast-furnace process. Metalurgija. 52, 197-200.

Birol, B., 2019. Investigating the utilization of blast furnace flue dusts and mill scale as raw materials in iron nugget production. Mater. Res. Express 6. 0865d1. DOI:10.1088/2053-1591/ab243b.

Brocchi, E.A., Moura, F.J., 2008. Chlorination methods applied to recover refractory metals from tin slags. Miner. Eng. 21 (2), 150-156. DOI:10.1016/j.mineng.2007.08.011.

Cantarino, M.V., De Carvalho Filho, C., Borges Mansur, M., 2012. Selective removal of zinc from basic oxygen furnace sludges. Hydrometallurgy 111–112, 124–128. DOI:10.1016/j.hydromet.2011.11.004.

Chatterjee, A., 2012. Sponge Iron Production by Direct Reduction of Iron Oxide, 2nd Ed. PHI Learning Limited, Delhi, India. ISBN: 978-8120346598.

Durinck, D., Jones, P.T., Blanpain, B., Wollants, P., Mertens, G., Eisen, J., 2007. Slag solidification modeling using the Scheil-Gulliver assumptions. J. Am. Ceram. Soc. 90,

1177–1185. DOI:10.1111/j.1551-2916.2007.01597.x.

ENDS Report, 1992. Scottish steel works leaves massive clean-up bill. ENDS Rep. No.215, 7.

Feild, A., 1917. The viscosity of blast-furnace slag and its relation to iron metallurgy, including a description of a new method of measuring slag viscosity at high temperatures. Trans. Faraday Soc. 13, 3–35. DOI:10.1039/TF9171300003

Fisher, L. V, Barron, A.R., 2019. The recycling and reuse of steelmaking slags — A review. Resour. , Conserv. Recycl. 146, 244–255. DOI:10.1016/j.resconrec.2019.03.010

Geerdes, M., Chaigneau, R., Kurunov, I., Lingiardi, O., Ricketts, J., 2015. Modern blast furnace ironmaking: an introduction, 3rd ed. IOS Press, Amsterdam, Netherlands. ISBN:978-1607500407.

Han, H., Duan, D., Chen, S., Yuan, P., 2015. Mechanism and influencing factors of iron nuggets forming in rotary hearth furnace process at lower temperature. Metall. Mater. Trans. B Process Metall. Mater. Process. Sci. 46, 2208–2217. DOI:10.1007/s11663-015-0420-0.

Han, J., Liu, W., Zhang, T., Xue, K., Li, W., Jiao, F., Qin, W., 2017. Mechanism study on the sulfidation of ZnO with sulfur and iron oxide at high temperature. Nature 7, 42536. DOI:10.1038/srep42536.

Horckmans, L., Nielsen, P., Dierckx, P., Ducastel, A., 2019. Recycling of refractory bricks used in basic steelmaking: A review. Resour. Conserv. Recycl. 140, 297-304. DOI:10.1016/j.resconrec.2018.09.025

Ishiwata, N., Sawa, Y., Hiroha, H., Matsui, T., Murao, A., Higuchi, T., Takeda, K., 2009. Investigation of reduction and smelting mechanism in the Hi-QIP process 80, 523–529. DOI:10.2374/SRI09SP040.

Jha, M.K., Kumar, V., Singh, R.J., 2001. Review of hydrometallurgical recovery of zinc from industrial wastes. Resour. Conserv. Recycl. 33 (1), 1–22. DOI:10.1016/S0921-3449(00)00095-1.

Kikuchi, S., Ito, S., Kobayashi, I., Tsuge, O., Tokuda, O., Midrex Technologies, I., 2010. ITmk3 process. Kobelco Technol. Rev. 29, 69–77.

Kobe Steel ltd, 2010. World's first commercial ITmk3 plant successfully begins production [WWW Document]. URL http://www.kobelco.co.jp/english/releases/2010/1182907_14776.html (accessed 5.29.18).

Liang, S., Liang, X., Tang, Q., 2020. Treatment of secondary dust produced in rotary hearth furnace through alkali leaching and evaporation-crystallization processes. Processes 8, 1–15. DOI:10.3390/PR8040396

Longbottom, R., Monaghan, B.J., Zhang, G., Chew, S., Pinson, D.J., 2016. Characterization of steelplant by-products to realise the value of Fe and Zn. Proc. 7th European Coke and Ironmaking Congress (ECIC 2016). Linz, Austria, 1017-1026.

Mager, K., Meurer, U., Garcia-Egocheaga, B., Goicoechea, N., Rutten, J., Saage, W., Simonetti, F., 2000. Recovery of zinc oxide from secondary raw materials: new developments of the Waelz process. Fourth Int. Symp. Recycl. Met. Eng. Mater. 329–344. DOI:10.1002/9781118788073.ch29.

McClelland, J.M., Metius, G.E., 2003. Recycling ferrous and nonferrous waste streams with FASTMET. Jom 55, 30–34. DOI:10.1007/s11837-003-0101-3

Memoli, F., 2015. Behavior and benefits of high-Fe3C DRI in the EAF, in: AIST, 2 (4), 1928–1945.

Mombelli, D., Di Cecca, C., Mapelli, C., Barella, S., Bondi, E., 2016a. Experimental analysis on the use of BF-sludge for the reduction of BOF-powders to direct reduced iron (DRI) production. Process Saf. Environ. Prot. 102, 410–420. DOI:10.1016/j.psep.2016.04.017.

Mombelli, D., Mapelli, C., Barella, S., Di Cecca, C., Le Saout, G., Garcia-Diaz, E., 2016b. The effect of microstructure on the leaching behaviour of electric arc furnace (EAF) carbon steel slag. Process Saf. Environ. Prot. 102, 810–821. DOI:10.1016/j.psep.2016.05.027.

Mombelli, D., Mapelli, C., Barella, S., Gruttadauria, A., Spada, E., 2019. Jarosite wastes reduction through blast furnace sludges for cast iron production. J. Environ. Chem. Eng. 7. DOI:10.1016/j.jece.2019.102966.

Narita, K., Onoye, T., Satoh, Y., Miyamoto, M., Taniguchi, K., Kamatani, S., Sato, T.,

Fukihara, S., 1981. Effects of alkalis and zinc on the wear of blast furnace refractories and the tuyere displacement. Trans. Iron Steel Inst. Japan 21, 839–845. DOI:10.2355/isijinternational1966.21.839.

Oustadakis, P., Tsakiridis, P.E., Katsiapi, A., Agatzini-Leonardou, S., 2010. Hydrometallurgical process for zinc recovery from electric arc furnace dust (EAFD). Part I: Characterization and leaching by diluted sulphuric acid. J. Hazard. Mater. 179, 1–7. DOI:10.1016/j.jhazmat.2010.01.059.

Pehlke, R.D., Fuwa, T., 1985. Control of sulphur in liquid iron and steel. Int. Met. Rev. 30, 125–140. DOI:10.1179/imtr.1985.30.1.125.

Sawa, Y., Yamamoto, T., Takeda, K., Itaya, H., 2001. New coal based process to produce high quality DRI for the EAF. ISIJ Int. 41, 17–21. DOI:10.2355/isijinternational.41.Suppl_S17.

Schrama, F.N.H., Beunder, E.M., Van den Berg, B., Yang, Y., Boom, R., 2017. Sulphur removal in ironmaking and oxygen steelmaking. Ironmak. Steelmak. 44, 333–343. DOI:10.1080/03019233.2017.1303914.

Seetharaman, S., 2014. Future of Process Metallurgy, in: Treatise on Process Metallurgy, Vol. 3: Industrial Processes. Elsevier, Amsterdam, Netherlands. 1563–1726. DOI:10.1016/B978-0-08-096988-6.00037-7.

Shawabkeh, R.A., 2010. Hydrometallurgical extraction of zinc from Jordanian electric arc furnace dust. Hydrometallurgy 104, 61–65. DOI:10.1016/j.hydromet.2010.04.014.

Simmons, J., 2015. E-Iron Nugget Process, in: CIM Montreal. Canadian Institute of Mining, Metallurgy and Petroleum, Montreal.

Song, S., Zhao, J., Pistorius, C.P., 2020. Communication MgO refractory attack by transient non-saturated slag. Metall. Mater. Trans. B 51, 891–897. DOI:10.1007/s11663-020-01788-x.

Sosinsky, D.J., Sommerville, I.D., 1986. The composition and temperature dependence of the sulfide capacity of metallurgical slags. Metall. Trans. B 17, 331–337. DOI:10.1007/BF02655080.

Srivastava, U., 2014. Sustainable Iron Making Process. PhD Thesis, Michigan Technological

University.

Srivastava, V.C., Mall, I.D., Mishra, I.M., 2006. Characterization of mesoporous rice husk ash (RHA) and adsorption kinetics of metal ions from aqueous solution onto RHA. J Hazard Mater. 134, 257–267. DOI:10.1016/j.jhazmat.2005.11.052.

Stewart, D.J.C., Barron, A.R., 2020. Pyrometallurgical removal of zinc from basic oxygen steelmaking dust – A review of best available technology. Resour. Conserv. Recycl. 157, 104746. DOI:10.1016/j.resconrec.2020.104746.

Strandkvist, I., Pålsson, K., Andersson, A., Olofsson, J., Lennartsson, A., Samuelsson, C., Engström, F., 2020. Minimizing chromium leaching from low-alloy electric arc furnace (EAF) slag by adjusting the basicity and cooling rate to control brownmillerite formation. Appl. Sci. 10. DOI:10.3390/app10010035.

Taniguchi, Y., Wang, L., Sano, N., Seetharaman, S., 2012. Sulfide capacities of CaO-Al_2O_3-SiO_2 slags in the temperature range 1673 K to 1773 K (1400 °C to 1500 °C). Metall. Mater. Trans. B Process Metall. Mater. Process. Sci. 43, 477–484. DOI:10.1007/s11663-011-9621-3.

Trung, Z.H., Kukurugya, F., Takacova, Z., Orac, D., Laubertova, M., Miskufova, A., Havlik, T., 2011. Acidic leaching both of zinc and iron from basic oxygen furnace sludge. J. Hazard. Mater. 192, 1100–1107. DOI:10.1016/j.jhazmat.2011.06.016.

Tsutsumi, H., Yoshida, S., Tetsumoto, M., 2010. Features of FASTMET Process. Kobelco Technol. Rev. 29, 85–92.

Umadevi, T., Brahmacharyulu, A., Karthik, P., Mahapatra, P.C., Prabhu, M., Umadevi, T., Brahmacharyulu, A., Karthik, P., Mahapatra, P.C., Prabhu, M., 2013. Recycling of steel plant mill scale via iron ore sintering plant. Ironmak. Steelmak. 39, 222–227. DOI:10.1179/1743281211Y.0000000063.

Wang, W., Xue, Z., Ma, G., 2010. Producing iron nuggets with Steel Making Wastes, in: 4th International Conference on Bioinformatics and Biomedical Engineering, Chengdu, China. pp. 1–4. DOI:10.1109/ICBBE.2010.5518019.

Wei, G., Zhu, R., Tang, T., Dong, K., 2019. Study on the melting characteristics of steel scrap in molten steel. Ironmak. Steelmak. 46, 609–617.

DOI:10.1080/03019233.2019.1609738.

Yao, Z.T., Ji, X.S., Sarker, P.K., Tang, J.H., Ge, L.Q., Xia, M.S., Xi, Y.Q., 2015. A comprehensive review on the applications of coal fly ash. Earth-Science Rev. 141, 105–121. DOI:10.1016/j.earscirev.2014.11.016.

Yellishetty, M., Mudd, G.M., Ranjith, P.G., Tharumarajah, A., 2011. Environmental life-cycle comparisons of steel production and recycling : sustainability issues , problems and prospects. Environ. Sci. Technol. 4, 650–663. DOI:10.1016/j.envsci.2011.04.008.

Zeydabadi, B.A., Mowla, D., Shariat, M.H., Kalajahi, J.F., 1997. Zinc recovery from blast furnace flue dust. Hydrometallurgy 47, 113–125. DOI:10.1016/S0304-386X(97)00039-X.

Zhang, D., Zhang, X., Yang, T., Rao, S., Hu, W., Liu, W., Chen, L., 2017. Selective leaching of zinc from blast furnace dust with mono-ligand and mixed-ligand complex leaching systems. Hydrometallurgy 169, 219–228. DOI:10.1016/j.hydromet.2017.02.003.

Zhao, D.N., Xue, Z.L., Wang, W., Li, Y.S., Song, S.Q., 2012. Process analysis of Pb and Zn during producing iron nuggets by iron bearing dust, in: Adv. Mat. Res. 402, 173–178. DOI:10.4028/www.scientific.net/AMR.402.173.

Zheng, Y.X., Lv, J.F., Wang, H., Wen, S.M., Pang, J., 2018. Formation of zinc sulfide species during roasting of ZnO with pyrite and its contribution on flotation. Sci. Rep. 8, 1–10. DOI:10.1038/s41598-018-26229-3.